Disclaimer

This is a reviewed problem set for the module physics601.

This problem set was reviewed by a tutor. *This does not mean that it is a perfect solution. Neither I or the tutor imply that there are no further mistakes in this document.*

All problem sets for this module can be found at
http://martin-ueding.de/de/university/msc_physics/physics601/.

If not stated otherwise in the document itself: This work by Martin Ueding is licensed under a Creative Commons Attribution-ShareAlike 4.0 International License.

[disclaimer]

Lab report

Magneto-optical trap

Experiment A248 – Universität Bonn

Martin Ueding
mu@martin-ueding.de

Lino Lemmer
l2@uni-bonn.de

2016-04-25 to 26

In this experiment we set up a magneto-optical trap to catch rubidium atoms. After that we investigate basic properties of the trap and its components.

We construct a MOT with 192(19) nW observable fluorescence power, $2.0(5) \times 10^7$ atoms trapped and a volume of 26.3 mm^3. The loading time of our trap will be determined to be 0.087(4) s. We compute the rubidium scattering cross section to be $2.1(3) \times 10^{-17}$ m^2.

Contents

1 Theory **5**

1.1 Optical cooling . . . 5
1.1.1 Radiation pressure . . . 5
1.1.2 Red detuning . . . 5
1.1.3 Optical molasses . . . 5
1.2 Magneto-optical trap . . . 6
1.3 Rubidium . . . 7
1.4 Diode lasers . . . 7
1.5 Doppler-free spectroscopy . . . 8
1.6 Polarization spectroscopy . . . 8

2 Conduction **10**

2.1 Apparatus . . . 10
2.2 Setup and calibration . . . 12
2.3 MOT characterization . . . 14
2.3.1 Lens configuration . . . 14
2.3.2 Fluorescence power . . . 15
2.3.3 Beam intensity . . . 15
2.3.4 Detuning of the laser frequencies . . . 16
2.3.5 Number of atoms . . . 18
2.3.6 Size of MOT . . . 20
2.3.7 Influence of quarter waveplates . . . 22
2.3.8 Influence of magnetic field . . . 22
2.3.9 Loading behavior . . . 23
2.3.10 Rubidium cross section . . . 23

3 Conclusion **26**

Permission to upload

I, Martin Ueding, would like to scan and upload this lab report with your corrections to my website martin-ueding.de. There, the original lab report as well as the reviewed one will be licensed under the "Creative Commons Attribution-ShareAlike 4.0 International License". Is that okay with you?

Yes ☒ No ☐

↳ "reviewed one" = you correct everything I note or plain scan of this report?

1 Theory

1.1 Optical cooling

1.1.1 Radiation pressure

Light, being mediated by massless gauge bosons, has a linear dispersion relation $E = cp$ with momentum $p = \hbar k$ and wave number k. An atom which absorbs a photon will obtain its energy and also its momentum. While in stimulated emission the momentum of the emitted photon points in the same direction as the stimulating atom's momentum, spontaneous emission is isotropic which leads to a net acceleration. This effect causes the so called radiation pressure.

1.1.2 Red detuning

To cool atoms down one has to make sure that only those atoms that move towards the laser beam feel this pressure. This can be done using the Doppler effect: In the rest system of the atom, that flies towards the laser beam, the photons of the laser are blue detuned, with $\nu' = \nu(1+v/c)$, where v is the velocity of the atom. To get those atoms on resonance again one has to detune the laser to the red.

1.1.3 Optical molasses

The force of a laser with intensity I and detuning $\Delta = \omega_{\text{laser}} - \omega_{\text{res}}$ on an atom can be expressed as

$$F_{\text{radiation}} = \frac{\hbar k \Gamma}{2} \cdot \frac{I/I_S}{\left(2\frac{\Delta - kv}{\Gamma}\right)^2 + 1 + I/I_S},$$

where k denotes the wave vector of the photons, Γ the decay rate of the excited state and I_S the saturation intensity. If we want to cool the force at $v = 0$ should be zero, which is clearly not the case. To solve this one uses two counterpropagating laser beams with the same detuning. For small velocities this gives a force depending force:

$$F_{\text{count}} = \frac{8\hbar k^2 \Delta}{\Gamma} \frac{I/I_S}{\left((2\Delta/\Gamma)^2 + 1 + I/I_S\right)^2} \cdot v \underset{\delta<0}{=} -\alpha \cdot v\,.$$

Applying three orthogonal pairs of lasers gives an effective deceleration of atoms in every direction and with this a cooling. This setup is known as *optical molasses*. This cooling process is

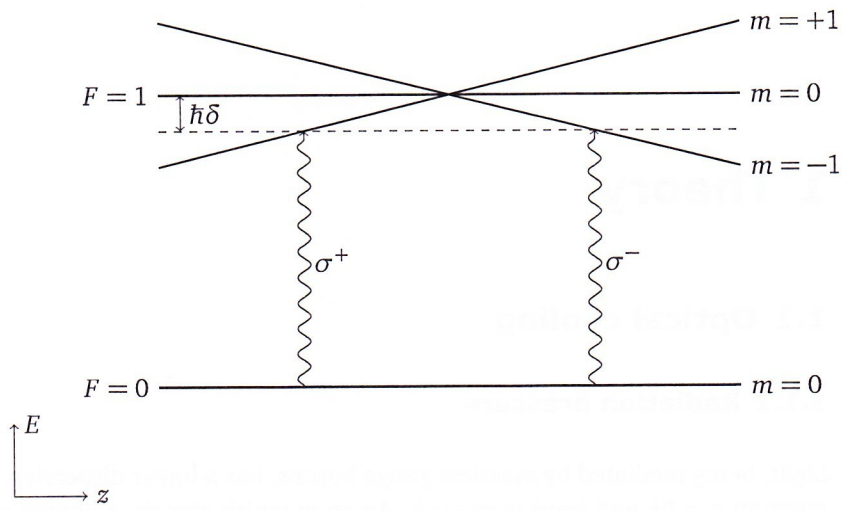

Figure 1.1: Energy levels and transitions in a spatially varying magnetic field.

limited by heating due to spontaneous emission. This leads to the so called *Doppler limit*

$$T_{\text{Doppler}} = \frac{\hbar\Gamma}{2k_{\text{B}}}.$$

1.2 Magneto-optical trap

Since the forces in the optical molasses are independent of space, the atoms diffuse out of the cooling area. Due to collisions those atoms get heated up again. We need an additional force that keeps the atoms inside that area. One possibility is to use a *magneto optical trap* (MOT).

To simplify the working principle we consider a two level system with one possible transition ($F = 0 \rightarrow F = 1$). Also we add a 1-dimensional linear increasing magnetic field without loss of generality along the z axis, which is zero at $z = 0$. Due to the Zeeman effect we get a space-dependent energy splitting of the three possible $F = 1$ configurations, which causes a lowering of the $m = 1$ state's energy for $z < 0$ and a lowering of the $m = -1$ level for $z > 0$ (see Figure 1.1).

Now we add two counterpropagating laser beams with detuning $\Delta < 0$. If now the laser beam propagating in positive z direction has a σ^+ helicity and the counterpropagating beam has a σ^- helicity, atoms which are located at $z < 0$ have a higher possibility to absorb σ^+ photons and hence get pushed back to $z = 0$. For atoms at $z > 0$ it is the other way around. There the absorption of a σ^- photon is more likely, so that they also get pushed back to $z = 0$.

While in reality the energy levels are way more complex the working principle remains the same.

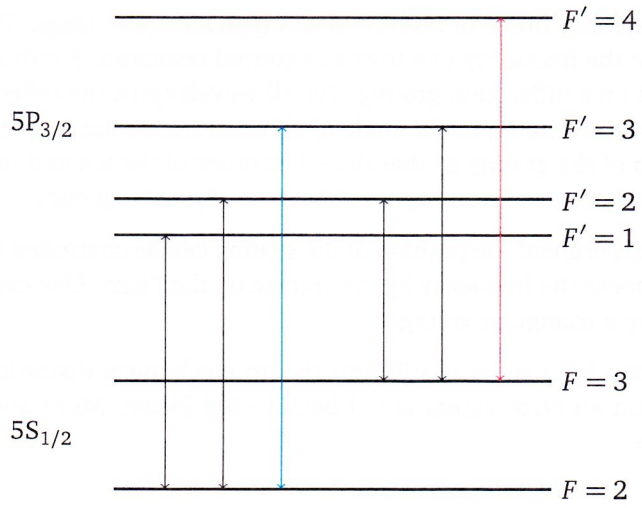

Figure 1.2: Part of the ^{85}Ru level scheme. The colored transitions are the ones used in this experiment. The cooling beam uses the red transition while the blue transition is needed for the repumping.

1.3 Rubidium

typically ^{85}Rb

Natural rubidium consists about 72 % of ^{85}Ru and 28 % of ^{87}Ru. In our MOT we use the former. Part of its hyperfine level scheme is shown in Figure 1.2. To create a quasi two level system we use the closed $F = 3 \rightarrow F' = 4$ transition. Since this is not a real two level system there is a finite probability for the transition from $F' = 4$ to $F = 2$. In this state the atom cannot be excited by the cooling laser again. Therefore it is called *dark state*. To solve this problem a second laser, the *pumping laser*, excites the atoms in the dark state to the $F' = 3$ state, from where it can decay into the cooling ground state $F = 3$ again and with this get the atom back in the cooling cycle.

→ normally we excite from $F=3$ to $F'=4$ and decay back (closed transition), but there are off-resonant excitations from $F=3$ to $F'=3$ and even $F'=2$ which can decay into $F=2$ (the decay from $F'=4$ to $F=2$ directly is strongly suppressed)

1.4 Diode lasers

A diode laser is a semiconductor diode, which works quite similar to a LED. Photons are produced in a highly doped p-n-junction by recombination of electrons and holes. Due to partial reflection at the border between diode material and the surrounding air the diode becomes a resonator, which works as laser if more atoms are excited rather than in their ground state. This can be reached by electrical pumping with a current in forward direction of the diode. The frequency of the laser depends on the size of the band gap. Because of the large active region this so called *homojunction laser diode* is very ineffective as it needs a high current density.

For our case the better diode is a so called *double-heterojunction laser diode*, which consists of a thin layer of low band gap material, sandwiched between two high band gap layers. This type requires a lower current density, which allows continuous wave operation at room temperature.

The frequency range of laser diodes is typically quite large. To get a narrow line width and to stabilize the frequency one uses an external resonator. For this the (divergent) laser beam gets focused on a diffraction grating. For all wavelengths the reflected beam of 0-th order points in the same direction, but the angle of all other orders are frequency dependent. One chooses the position of the grating so that the -1-st order of the wanted frequency is coupled back into the laser, which causes a strong amplification of that frequency.

In this experiment the position of the grating can be controlled with a Piezo element. This allows us to choose the frequency by the voltage on the Piezo. One can now scan trough frequencies by applying a triangular voltage.

The diode laser setup is still sensitive to mechanical distortions. For a further frequency stabilization an error signal is fed back to the Piezo. More about this error signal in the next sections.

1.5 Doppler-free spectroscopy

Since the Doppler broadening of spectral lines at room temperature is orders of magnitude bigger than the natural line width, lines which lie close together cannot be resolved. To nevertheless investigate those lines one has to use Doppler-free spectroscopy.

For this two counterpropagating laser beams of the same frequency are needed, a *pump beam* and a *probe beam* with lower intensity. The absorption of the probe beam gets recorded. For a simple understanding again consider a two level system with ground state $|g\rangle$, excited state $|e\rangle$ and energy difference of $\hbar\omega_0$. If the lasers both have the frequency ω_0 atoms with $v \neq 0$ along the laser's direction will be out of resonance due to the Doppler effect. Those atoms with $v \approx 0$ will be excited by the pump beam and hence the absorption of the probe beam is very low. If the lasers are detuned to the red from the resonance frequency the pump beam and the probe beam excite oncoming atoms with respect to their own propagation direction. Therefor the absorption of the probe beam is high. The same holds for blue detuned lasers. This leads to a transmission spectrum as in Figure 1.3a. If one takes an absorption spectrum one gets dips instead of peaks, which are called *Lamb dips*.

In reality there will be more levels, which makes the absorption spectrum more complex. Take for example a system with one ground level and two excited level with excitation energy $\hbar\omega_1$ and $\hbar\omega_2$ respectively. When we apply the same method as above it can happen that the pump beam is on resonance with one of the excited levels and the probe beam with the other. This leads to a so called *cross over peak* at $\omega_{\text{probe}} = (\omega_1 + \omega_2)/2$ (see Figure 1.3b).

1.6 Polarization spectroscopy

The error signal for frequency stabilization can be obtained using polarization spectroscopy. As the name implies this kind of spectroscopy uses the probe beam's polarization rather than its intensity. The reason for this is that one can detect small changes in polarization much better than small changes in intensity.

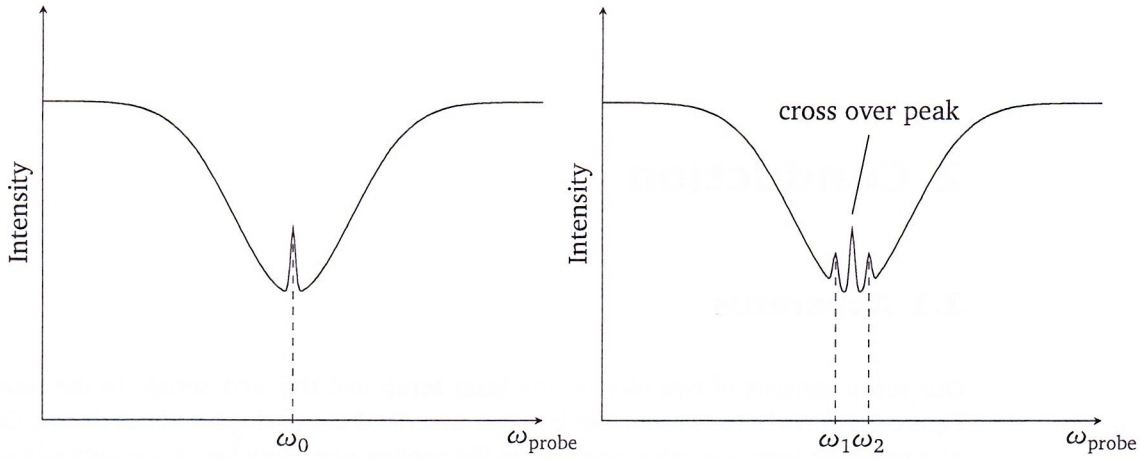

(a) Two level system. (b) Three level system.

Figure 1.3: Transmission spectra in Doppler-free spectroscopy.

Polarization spectroscopy uses a setup similar to the one of the Doppler free saturation spectroscopy. In contrast to the latter the pump beam is circular polarized. Additionally there are two linear polarizers, one at each end of the spectroscopy cell, which are crossed, so that the background signal is suppressed.

→ for detection of pol. axis shift rather than background suppression

Due to the circular polarized pumping beam ($\Delta m = \pm 1$) the degenerate m states of the transition's excited level get unequally occupied, which leads to an alignment different from the thermal equilibrium. The resulting anisotropy shifts the polarization axis of the linear probe beam, which hence can be detected. The precision is due to the crossed polarizers up to three orders of magnitude better than the precision of the saturation spectroscopy. If there is a small angle between the two beams and if the birefringence of the cell's windows is reduced one can obtain a signal with a dispersive profile which allows to detect small deviations of the wanted frequency. These can be used to correct the grating's angle so that the frequency lock remains stable.

also a polarizing beam splitter can be used for gaining two pol. dependent intensity signals which can be substracted to get the dispersive signal (as in this experiment)

2 Conduction

2.1 Apparatus

Our setup consists of two blocks: the laser setup and the MOT setup. In the laser setup (see Figure 2.1a) we have two tunable lasers as described in the chapter about theory. One will serve as a pumping laser, the other one will be the cooling one. Both lasers are optically isolated using a Faraday isolator. This relieves us from making sure that no light feeds back into the laser system. Without the isolator, we would create a second laser cavity which we do not want.

Each laser has an independent locking mechanism via polarization spectroscopy. Part of the laser beam is taken away with a polarizing beam splitter and analysed in a rubidium cell. The error signal from each laser is fed into a lock box (not shown) to lock the laser into the desired frequency.

The light of the two lasers is combined into an optical fiber which leads the light to the MOT setup shown in Figure 2.1b. There we split the light into three approximately equally powered beams using $\lambda/2$ plates and polarizing beam splitters. Each of the those three linearly polarized beams is sent through a $\lambda/4$ plate to become circularly polarized. That is then led through the MOT chamber and back again with reversed polarization.

An annotated photo of the MOT setup is shown in Figure 2.2. The colors of the beams are just to help the eye, the beam itself always had the same IR "color". The individual elements are the following.

1. Exit of optical fiber. The combined light of cooling and pumping laser enters the MOT part of the experiment here.
2. $\lambda/2$ plate. Adjusts the polarization of the light onto the beam splitter.
3. Polarizing beam splitter. Splits the linearly polarized light in order to use one beam in the z-direction and the remainder in the transversal direction. By adjusting the $\lambda/2$ plate ② in front, one can adjust the beam power splitting.
4. Mirror and $\lambda/4$ plate. Reflects the incoming light upwards through the MOT chamber. The plate then makes the light circularly polarized.
5. $\lambda/4$ plate.
6. Mirror. Reflects the light back down.
7. Mirror. Reflects one beam from ③ upwards.
8. Mirror. Directs the light back into the horizontal. ⑦ and ⑧ will be called "elevator" occasionally.
9. $\lambda/2$ plate. Allows to adjust the splitting ratio with ⑩.

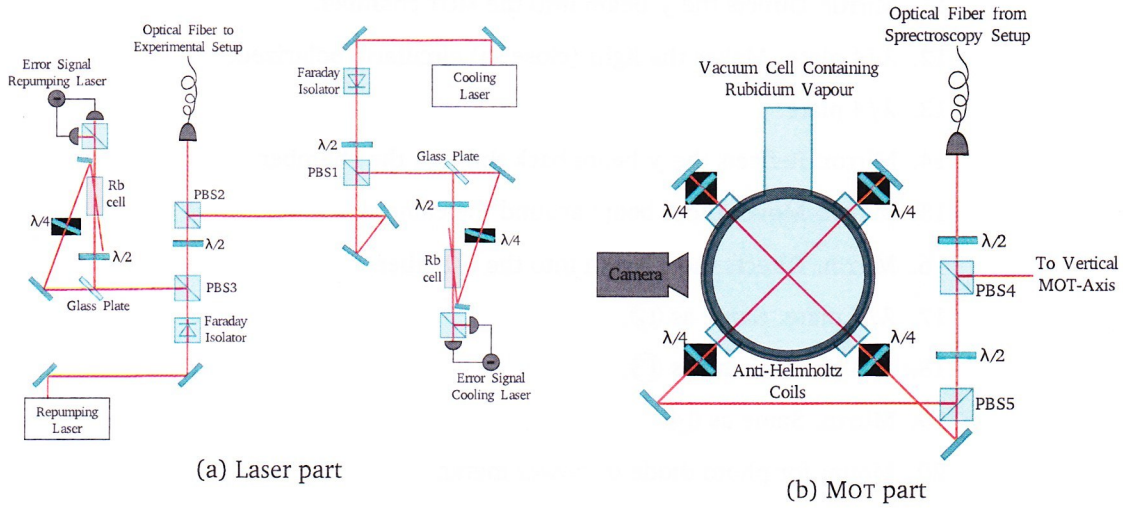

(a) Laser part

(b) MOT part

Figure 2.1: Setup of the experiment. Both images are taken from the supplementary material.

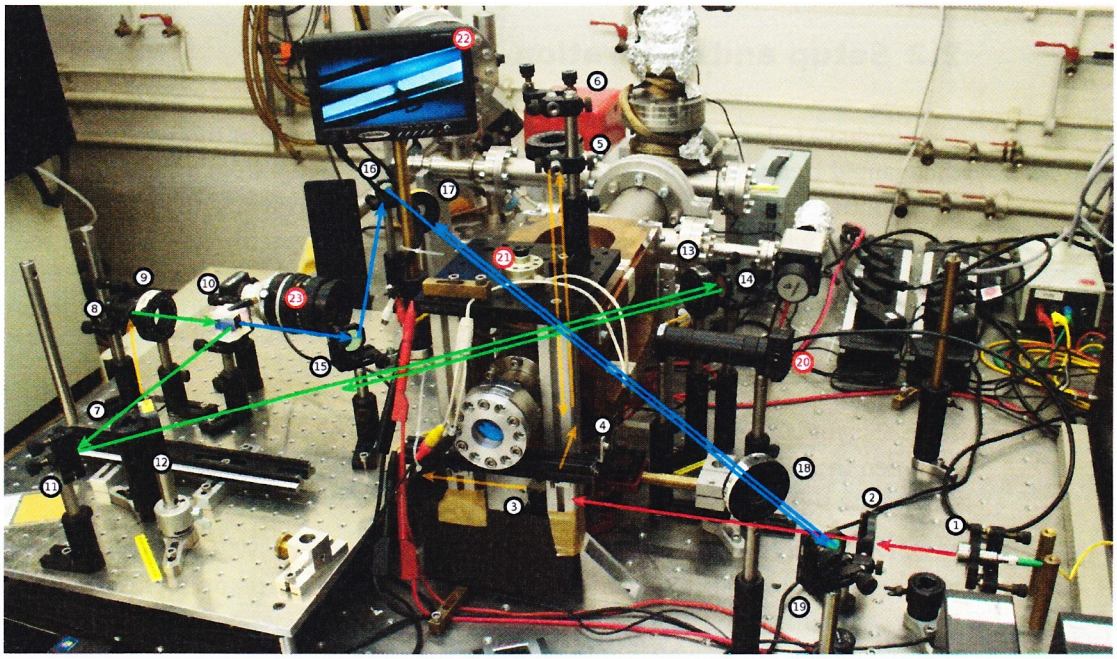

Figure 2.2: Setup of the MOT. The arrows show the path of the light rays. Ray colors are for illustration only. Numbers are explained in the text.

nice pic

10. Polarizing beam splitter. Splits the incoming beam into x (blue) and y (green) part.
11. Mirror. Directs the y beam into the MOT chamber.
12. $\lambda/4$ plate. Makes the light (close to) circularly polarized.
13. $\lambda/4$ plate.
14. Mirror. Reflects the y beam back through the chamber.
15. Mirror. Moves the x beam around the camera.
16. Mirror. Directs the x beam into the chamber.
17. $\lambda/4$ plate. Same as ⑫.
18. $\lambda/4$ plate. Same as ⑬.
19. Mirror. Same as ⑭.
20. Mount for photo diode or power meter.
21. IR camera. Useful for setting up the lasers.
22. Live screen for IR camera.
23. Camera directed onto MOT. Needed for MOT size estimation.

All the nine mirrors and three $\lambda/2$ have to be adjusted by us. The six $\lambda/4$ plates are set to a decent setting from the start.

2.2 Setup and calibration

First we have to lock the cooling laser to the right transition. For this we tune the laser roughly to the wanted frequency. The lock box gets a triangular signal from a function generator, changes its amplitude and offset and gives it to the piezo which controls the grating's position. On the oscilloscope we display the signal from the polarization spectroscopy cell and see the spectrum. That Doppler-free spectrum of the $F = 3$ ground state of ^{85}Ru is shown in Figure 2.3. From there we choose the right line, zoom in (reduce scanning amplitude) and lock the laser to a frequency a bit below the chosen transition.

For the pumping laser we repeat the last steps. The Doppler-free spectrum of the $F = 2$ ground state of ^{85}Ru is shown in Figure 2.4. The lines are so close together that we can not distinguish between them. Instead of trying to lock we quasi-lock by zooming in far to the spot where we expect the right transition to be.

Now we check if enough light is passing through the fiber. With the powermeter we measure a total power of 16.8 mW. Then be block the path of the pumping laser and measure again. Now we get 14.1 mW. The instruction states the cooling laser needs to be at least 5 mW and the pumping laser 1 mW, which both is clearly the case for our setup.

After that we have to adjust the polarizing beam splitter and the mirrors. For that we first check if the first PBS and the bottom elevator mirrors are hit nicely by the beam. After this is the case we modify the bottom z-mirror's orientation such that the beam passes through the center of the

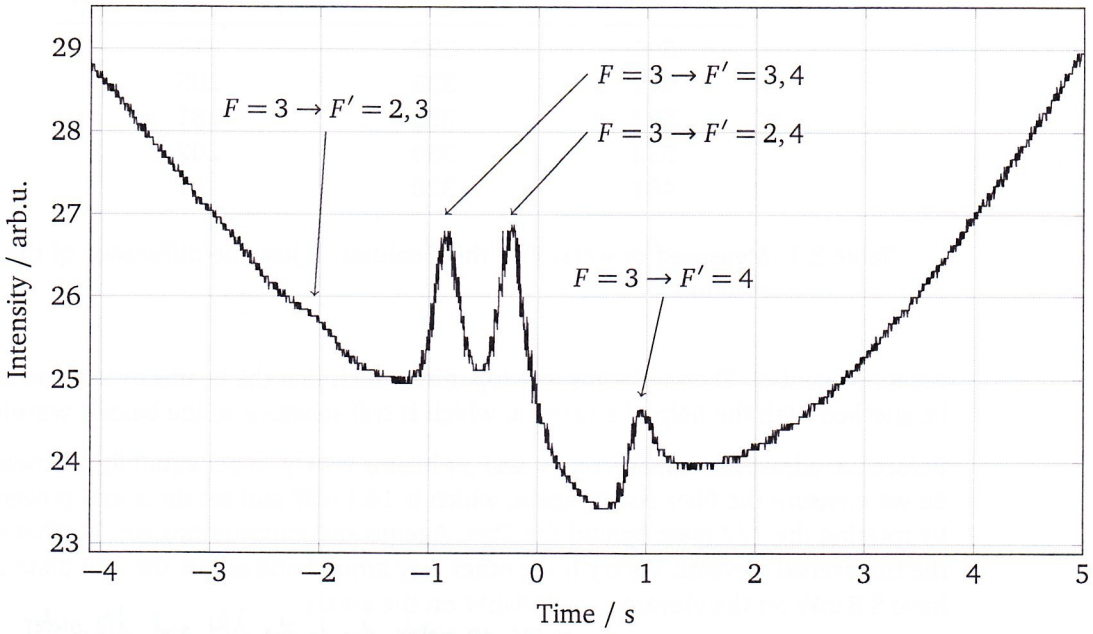

Figure 2.3: Doppler-free spectrum of the ^{85}Ru $F = 3 \rightarrow F' = 2,3,4$ lines. The time is related to the lasing frequency via the triangular voltage applied to the piezo.

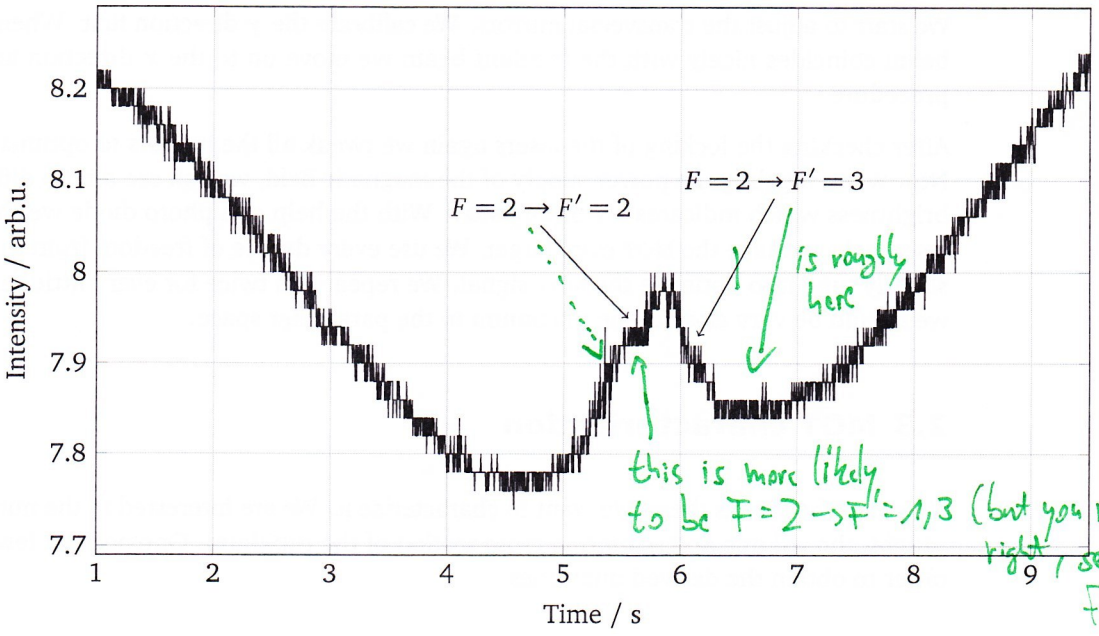

Figure 2.4: Doppler-free spectrum of the ^{85}Ru $F = 2 \rightarrow F' = 1,2,3$ lines. The time is related to the lasing frequency via the triangular voltage applied to the piezo. Since one can not distinguish between lines, the labels are only rough estimates.

total power/nW	background/nW	power of MOT/nW
550	337	213
543	338	205
503	322	181
532	330	202
481	320	161

Table 2.1: Measured powers. The third column is just the difference of the first two columns.

vacuum chamber. Then we adjust the top mirror such that the beams overlap perfectly. This can be checked with the help of a camera, which is still sensitive to the beam's wavelength.

Before we adjust the transversal (x and y) beams we try to get equal light power to each axis. So we measure the fiber power again, which is 15.1 mW and set the z-axis power to to 5.0 mW by rotating the $\lambda/2$ plate behind the fiber. Against our expectations we then have no power on the transversal elevator. We try it the other way around and adjust the $\lambda/2$ plate again until we have 8.8 mW on the elevator and 4.8 mW on the z-axis.

After measuring the beam power directly in front of the vacuum chamber we realize that we incur loss on all the mirrors and first adjust the splitting in the transversal directions to be symmetric. There now are 2.7 mW on each of them. Then we adjust the initial $\lambda/2$ plate to give more power to the transversal and less to the longitudinal direction. After that we have 3.1 mW behind each polarizing beam splitter.

We start to adjust the transversal mirrors. We calibrate the y direction first. When the reflected beam coincides nicely with the incident beam we move on to the x direction and repeat the procedure.

After checking the locking of the lasers again we tweak all the mirrors to optimize the overlap. Now when toggling the power supply of the magnetic field, we can see a little difference in the brightness which indicates a working MOT. With the help of a photo diode we then adjust the laser locks to make the MOT even larger. We use every degree of freedom from the mirrors and slightly tune it to optimize the MOT signal. We repeat this twice for every little screw such that we should be very close at the maximum in the parameter space.

2.3 MOT characterization

Now that the MOT is there, we want to characterize it. We are interested in the number of atoms caught, the volume and scattering cross section of the rubidium. One needs a few quantities in order to obtain the derived quantities.

2.3.1 Lens configuration

We need the diameter of the lens and its distance to the MOT. Since the lens is an 1 in lens, its radius is $d/2 = 1.27\,\text{cm}$. Its distance to the MOT is $l = 10(1)\,\text{cm}$, roughly estimated. Then we

absolute position/cm	power of beam/mW
28.8	3.35
29.0	3.36
29.2	3.30
29.3	3.06
29.4	2.43
29.5	1.60
29.6	0.800
29.7	0.260
29.8	0.100
30.0	0.003 00
30.2	0.002 00

Table 2.2: Measurement to estimate the beam diameter.

can work out the solid angle that is taken up by the lens. The solid angle is 4π for the whole sphere. Therefore we need to take the ratio of the lens surface ($\pi d^2/4$) and divide it by the total surface of a sphere at distance l, $4\pi l^2$. In total we will then obtain

$$\Omega = 4\pi \frac{\pi d^2}{16\pi l^2} = \frac{\pi d^2}{4l^2} = 0.05(1)\,\mathrm{sr}\,.$$

2.3.2 Fluorescence power

We then have to find the fluorescence power of the MOT. After replacing the photo diode with the powermeter, we see that our MOT is very bright but not very constant in power. Therefore we measure a few times to find a mean value (see Table 2.1). Our MOT's power is hence $p = 192(19)\,\mathrm{nW}$ which is quite good, as the instruction states that about 50 nW are needed.

With the solid angle we can convert the measured power p into the actual emitted power of the whole MOT, p_{tot}. We do this by dividing through the solid angle:

$$p_{\mathrm{tot}} = p\frac{4\pi}{\Omega} = 5(1) \times 10^4\,\mathrm{nW}\,.$$

2.3.3 Beam intensity

Then we need the beam's power. We measure on each axis separately and get $P_x = 3.57\,\mathrm{mW}$, $P_y = 3.36\,\mathrm{mW}$ and $P_z = 4.45\,\mathrm{mW}$.

Another quantity we have to know is the beam diameter. For this we put a razor blade on an optical rail in the y-beam and measure the remaining power depending on the razor's position. Our measurements are shown in Table 2.2.

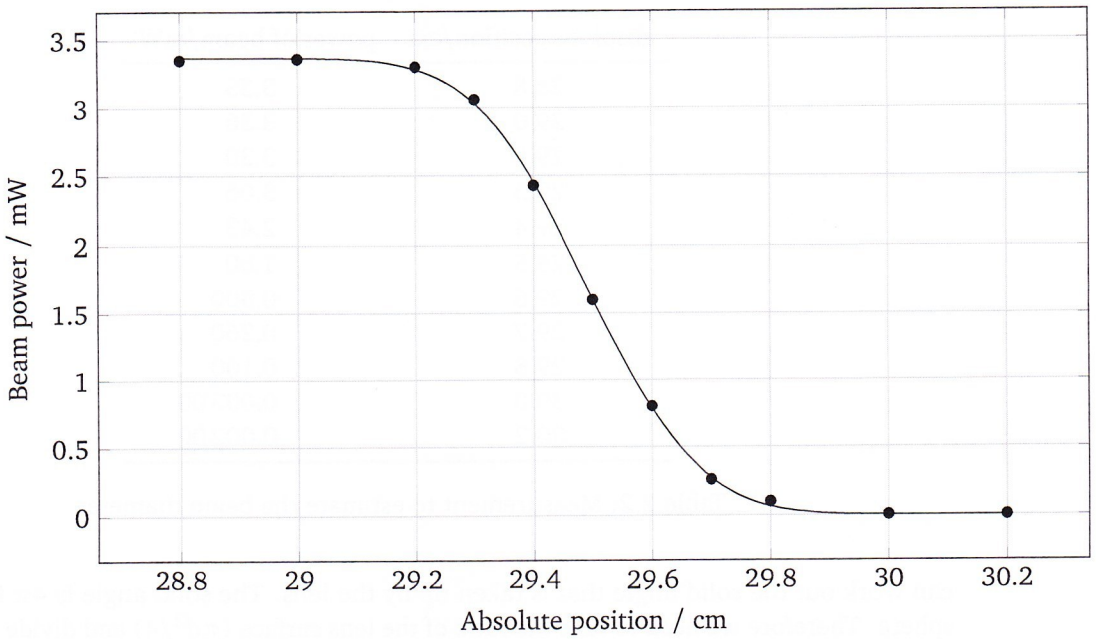

Figure 2.5: Beam diameter measurement. Shown is the beam power that is left after moving the razor blade to the given position.

The collected data is also shown in Figure 2.5 with a Gaussian CDF[1] fit. From the fit we derive a beam power of 3.37(1) mW for the y-branch and an e^{-2} beam diameter of 0.598(10) cm. Errors are estimated by the diagonal of the fit covariance matrix.

The beam intensity I is the total energy of the six beams (22.8 mW) divided by the cross sectional area of the beam, $\pi r^2 = 0.281(9)\,\mathrm{cm}^2$. We have

$$I = 2\frac{P_x + P_y + P_z}{\pi r^2} = 81(3)\,\mathrm{mW\,cm^{-2}},$$

where the factor two stems from the backreflection of each beam back through the chamber. With the intensity I we can build up give the scattering rate of an individual atom as given by Wieman, Flowers, and Gilbert [WFG95, Equation (4)] and already used in our theory chapter:

$$R = \frac{(I/I_s)\pi\Gamma}{1 + (I/I_s) + 4(\Delta/\Gamma)^2} = 9.3(2)\,\mathrm{MHz}.$$

The authors state the natural line width $\Gamma = 6\,\mathrm{MHz}$ and $I_s = 4.1\,\mathrm{mW\,cm^{-2}}$ Wieman, Flowers, and Gilbert [WFG95, p. 328]. We also need the wavelength $\lambda = 780\,\mathrm{nm}$. Using that we can compute $\hbar\omega = 2.55 \times 10^{-4}\,\mathrm{nW\,MHz^{-1}}$. The funny unit will become handy later on.

2.3.4 Detuning of the laser frequencies

So far we have tweaked the detuning of the cooling and repumping lasers in order to get the largest MOT. Now we want to investigate the MOT dependence on the detuning. First we unlock

[1] cumulative density function

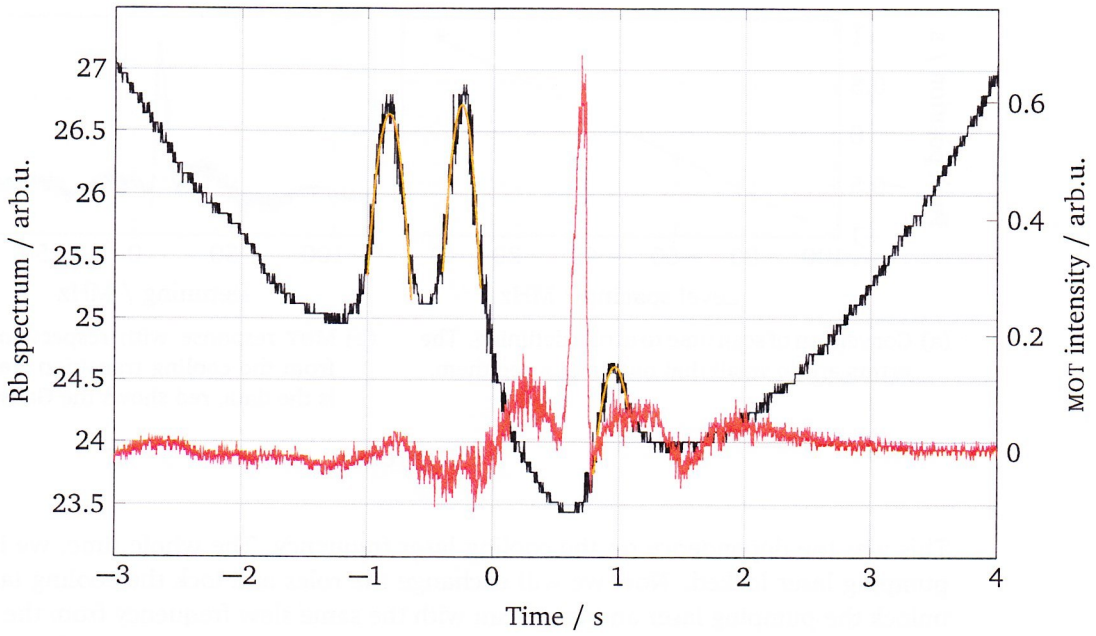

Figure 2.6: Scanning of the cooling laser. The rubidium spectrum of the cooling laser is shown in black. The red curve is the difference of photodiode signals with and without the magnetic field. One can see that the MOT forms only at the cooling transition. The thick orange lines are Gaussian fits to the peaks.

in the region red detuned of →

the cooling laser. Then we use the frequency generate to generate a 100 mHz triangular signal which we use as detuning of the cooling laser.

Using the photodiode, we can get fast feedback from the MOT. We attach the cooling laser rubidium spectrum signal and the photodiode to the oscilloscope. Then we set the trigger on the rising flank of the MOT signal. One spectrum with the magnetic field switched on is taken, another one without the field. This way we can subtract the background. The difference between the two MOT signals gives the intensity of the MOT itself. We plot that signal together this the rubidium spectrum, that is shown in Figure 2.6.

The time scale in that diagram is given by the scanning frequency chosen via the function generator. It is not really meaningful for our experiment. Therefore we identify three peaks in the rubidium spectrum. We fit a Gaussian curve to obtain the center of each peak. Then using the level shifts given in the second oscillogram from the appendix of the manual, we can obtain a connection between the scanning time and the detuning from the cooling transition. The three values used are shown in Figure 2.7a. We perform a linear fit and use this to convert the time scale into a frequency scale. Figure 2.7b shows the dependence of the MOT response (background already subtracted) with respect to the detuning frequency.

↳ Lorentzian might be a bit more precise, but ok

Performing a Gaussian fit to the MOT response peak, we can get a good estimate of the central value of that peak. This should be the detuning that we have used then we optimized the MOT for brightness in the previous steps. The Gaussian fit gives us a central value of $\Delta = -13.22(10)\,\text{MHz}$. ✓

↳ discussion: is this a reasonable result?

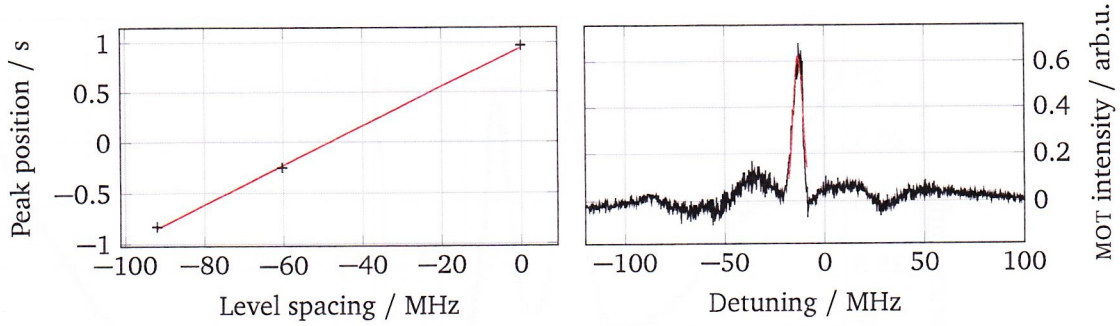

(a) Conversion of scan time to actual detuning. The errors are so small that one cannot see them.

(b) MOT response with respect to the detuning from the cooling transition frequency. Black is the data, red shows the Gaussian fit.

Figure 2.7

This was the dependence on the cooling laser frequency. The whole time, we have kept the pumping laser locked. Now we will exchange the roles and lock the cooling laser. Then we unlock the pumping laser and let it scan with the same slow frequency from the generator. In Figure 2.8 we show the rubidium spectrum and the MOT signal without background.

We would like to have done the same conversion of scanning time to detuning frequency. However, the peaks are too smeared out to perform a decent Gaussian fit. Therefore we cannot convert this into a detuning frequency. In the figure one can see that the greatest response in the MOT happens at the point where one would expect to see the repumping transition, that is between 0.6 s to 1.0 s on this scale.

ok!
$F=2 \to F'=3$ which is a little more efficient than the other one

2.3.5 Number of atoms

Now we have everything we need to compute the number of atoms in the MOT. The number of quantities going into this number is rather high, therefore see Figure 2.9 for a "flowchart" of the quantities used.

With a wavelength of the cooling laser λ we can compute the angular frequency ω and the photon energy $\hbar\omega$. Dividing the total power by the energy of a single photon gives us the total scattering rate

$$NR = \frac{4\pi p}{\Omega\hbar\omega}.$$

Dividing by the scattering rate we arrive at the expression for the atom number depending only on observables that we have:

$$N = \frac{4\pi p}{\Omega\hbar\omega}\frac{1+(I/I_s)+4(\Delta/\Gamma)^2}{(I/I_s)\pi\Gamma} = 2.0(5)\times 10^7.$$

✓

↳ short discussion if this is typical value?

because the detuning of the repumping laser should be roughly $\delta = 0$ for each transition you can estimate the position of the transitions in the spectrum by looking at the fluorescence peaks

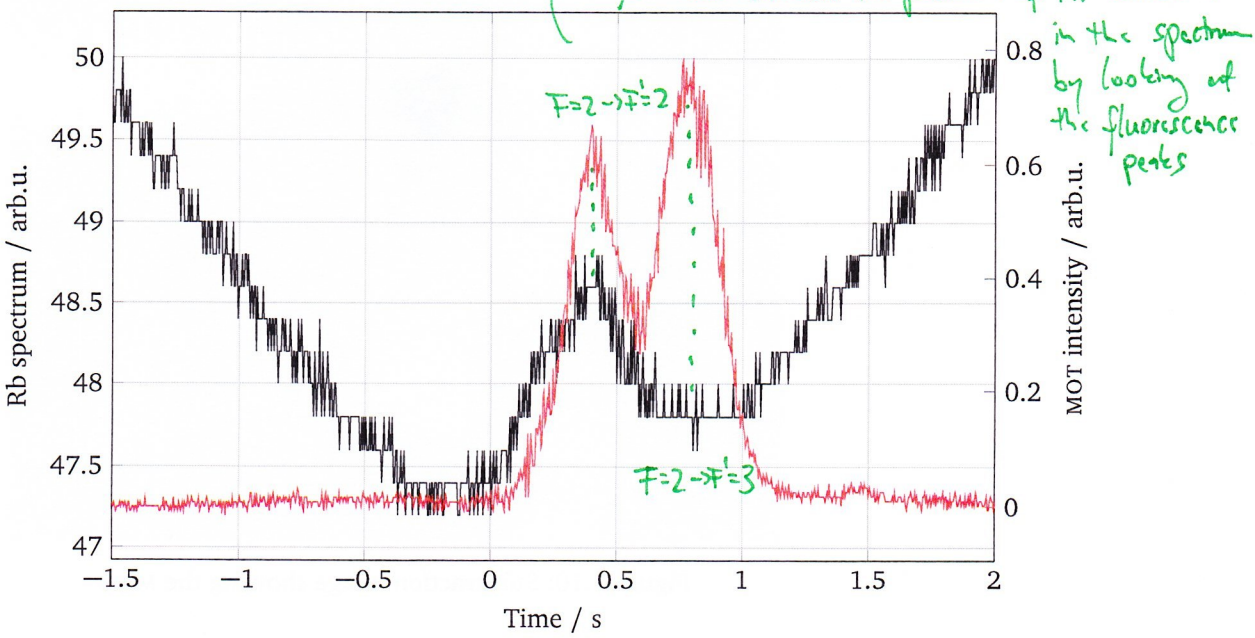

Figure 2.8: Scanning of the pumping laser. The rubidium spectrum of the pumping laser is shown in black. The red curve is the difference of photodiode signals with and without the magnetic field, i.e. the MOT signal.

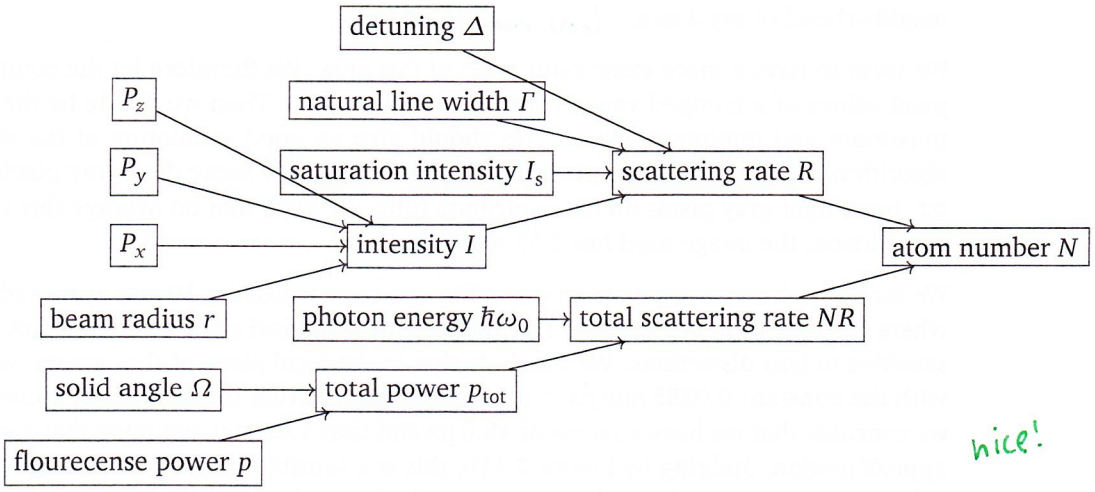

nice!

Figure 2.9: Conversion of quantities to obtain the MOT population.

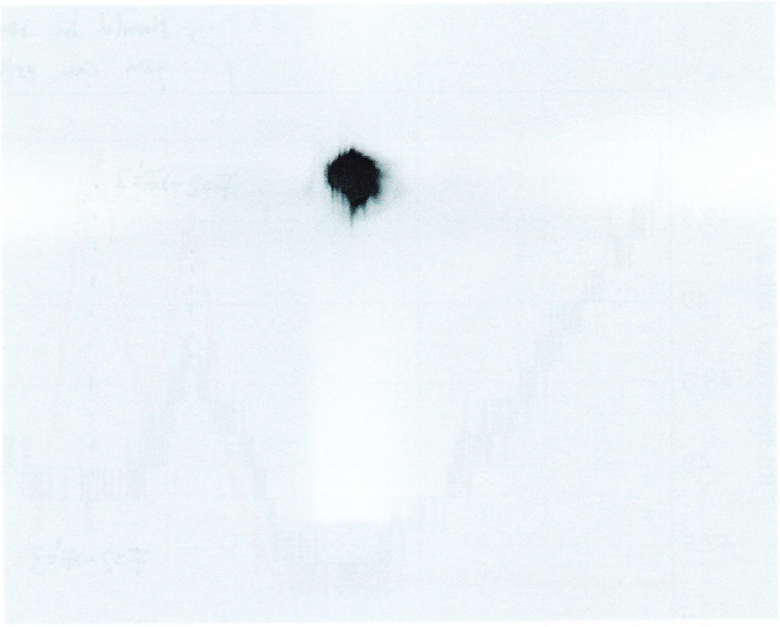

Figure 2.10: Substraction image showing the MOT.

2.3.6 Size of MOT

Now we want an estimate of our MOT's spatial size. For this we first take a picture of the chamber with the MOT and without it. Then we subtract those images in order to remove the background from the other laser beams. The subtracted image is shown in Figure 2.10.

Then we turn the camera and take a picture of a scale at the same distance. The image of the centimeter scale is shown in Figure 2.11a. For a rough estimation, the superposition of the MOT signal and the scale shown in Figure 2.11b can used. The radius of the MOT should be in the neighborhood of say 2 mm. looks more like 1,5 mm

We want to have a more exact estimation of this area. We therefore let the computer sum the pixel values of a cropped version shown in Figure 2.12. Then we divide by the difference in maximum and minimum value. This should give an good estimation of the MOT size. Our algorithm counts 7235 white pixels belonging to the MOT. Some dark gray pixels contribute a bit, some light gray pixels do not contribute fully. We hope that on average this works out. For comparison, the image used has 2.51×10^4 pixels.

We carefully choose two points on the millimeter scale which are 10 mm apart and near the spot where the MOT is on our images. This reduces the statistical error a bit while not becoming too sensitive to lens distortions. We conclude that in the focal plane of the camera, we can convert with the constant $0.0385\,\mathrm{mm\,px^{-1}}$ to physical sizes.[2] From the number of white pixels, 7235, we conclude that we have a radius of 48.0 px and thus 1.85 mm assuming that a circle is a good approximation. Judging by Figure 2.11b, this is a sensible result. Converting this radius to a volume, we obtain a spherical MOT volume of $26.3\,\mathrm{mm^3}$.

[2] px is the unit for pixels, at least in CSS (Cascading Style Sheets).

ok!

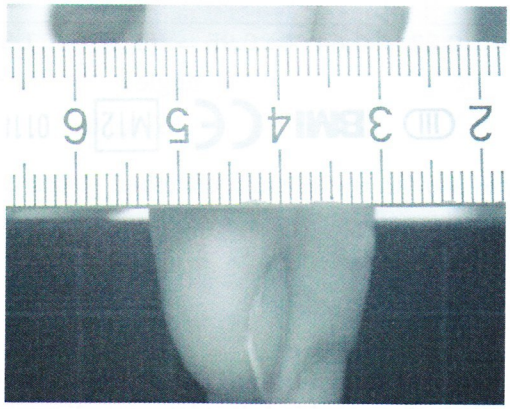

(a) Whole image of scale.

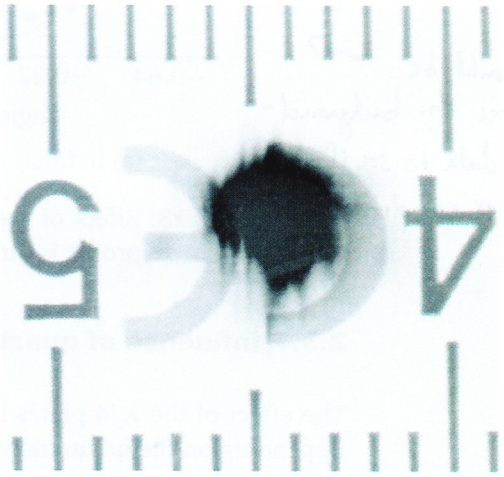

(b) Superposition of MOT and scale.

Figure 2.11: Millimeter scale at the same distance as the MOT.

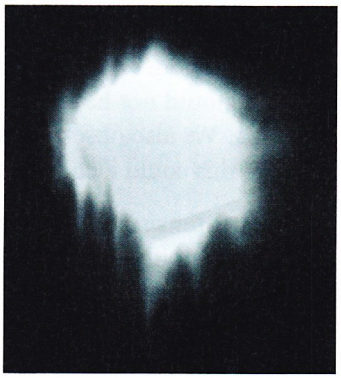

Figure 2.12: Selection used for area determination.

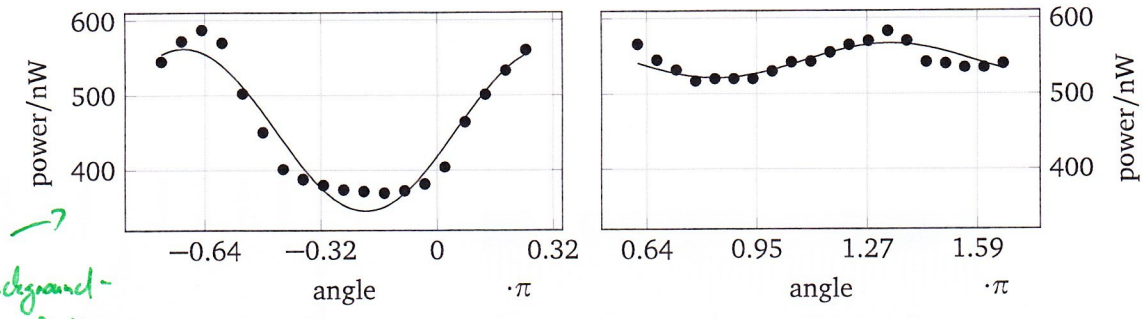

(a) In front (b) Behind

Figure 2.13: Effect of the $\lambda/4$ plates around the vacuum chamber. A $\cos(\phi - \phi_0)^2$ profile is fitted to the data.

2.3.7 Influence of quarter waveplates

The effect of the $\lambda/4$ plates in front of the MOT is significant. This is shown in Figure 2.13a. Depending on the orientation of the plates the beam behind the plate stays linearly or becomes elliptically or circularly polarized. This can suppress the formation of the trap completely. We have fitted a $\cos(\phi - \phi_0)^2$ function to the data as we expect the amplitude to scale with the cosine and the intensity with the square of that.

The effect of the plates in the backreflected beam can be seen in Figure 2.13b. It is not very large. Ideally there should be no change of the MOT's power, of course. The effect that we do see indicates that the light going through the MOT is not perfectly circularly polarized.

2.3.8 Influence of magnetic field

With the power meter still attached, we can investigate the influence of the external magnetic field onto the MOT power. We just vary the current that goes through the magnetic coils. In steps of around 0.5 A we take measurements. We first started with the maximum current and then go to no current. After that we measured a few more points in the middle. While doing this we noticed deviations from the previous measurements. This could be some mild hysteresis effect. In principle the copper coils should not have a strong ferromagnetism and therefore should not inhibit a significant hysteresis. We also observed large fluctuations of around 40 nW while taking the measurement. Therefore this could also be just statistical jitter that we have observed.

The dependence of the MOT intensity on the external magnetic field current is shown in Figure 2.14. One can see some sigmoidal shape here. Given the large errors of our measurement, one could perhaps also succeed with a linear fit. Nevertheless, a sigmoidal shape does make sense: For vanishing magnetic field, we do not expect to see a MOT signal, only some background from the optical molasses trapped for a very short time. Reversing the magnetic field should not make the signal go below 320 nW. Unfortunately, we did not test that.

A small magnetic field would give a small force and we would expect to see a smooth onset of some rising curve. At some magnetic field density, we have a deep potential to catch the atoms in. We will become limited by other parameters of the setup, for instance the beam overlap.

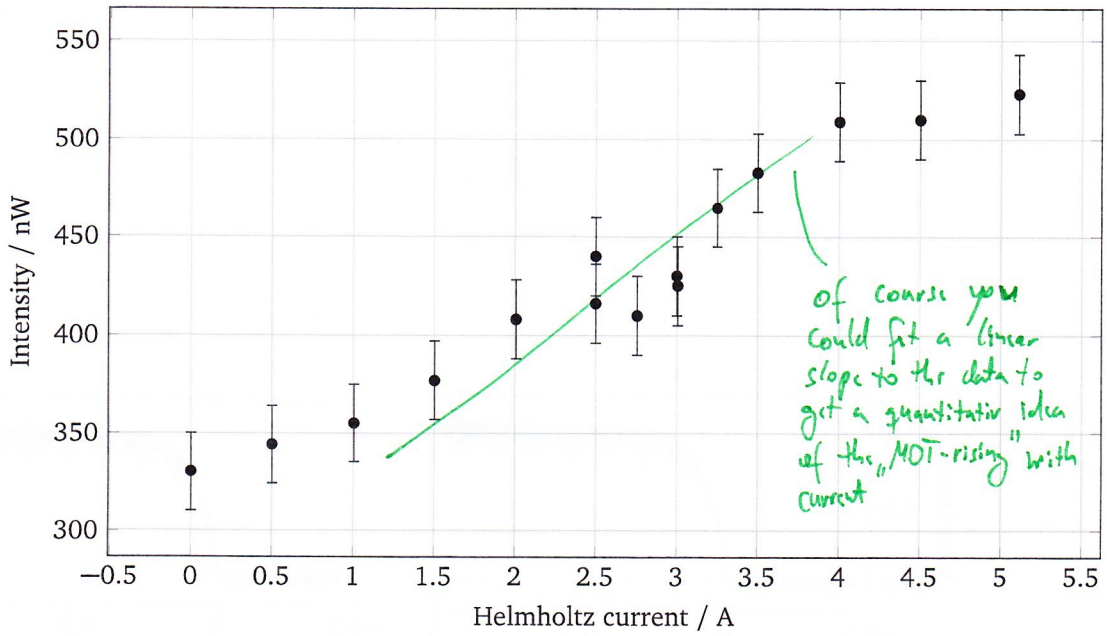

Figure 2.14: MOT response to a changing magnetic field. The points in the middle have been measured twice after we noticed some hysteresis effect.

Therefore the growing trend will have to stop for some magnetic field. It is expected to see two flat regimes connected by some smooth function. That will just be a sigmoidal shape. ✓

2.3.9 Loading behavior

To model the loading of the trap, we use a rising exponential with steady-state load N_0, start time t_0 and the "lifetime" in the filling process as given by Wieman, Flowers, and Gilbert [WFG95, Equation (1)]:

$$N(t) = N_0\left[1 - \exp\left(-\frac{t - t_0}{\tau}\right)\right].$$

Figure 2.15 shows four of six measurements that we did for the loading of the MOT. We have rescaled and shifted all signals from the photodiode such that one can easily compare the signals visually.

Fitting the function to our data from the rise of the signal, we obtain an average loading time of $\tau = 0.087(4)\,\mathrm{s}$. Judging from the plots, this is a reasonable result. ✓

2.3.10 Rubidium cross section

The pressure inside could not be measured during the experiment as the device was broken. Therefore we were given the pressure to lie in the range 1.1×10^{-7} mbar to 1.5×10^{-7} mbar. Therefore we will use $P = 1.3(2) \times 10^{-5}$ Pa for our calculations. The error is just the standard deviation of both points. The room temperature has been 24 °C.

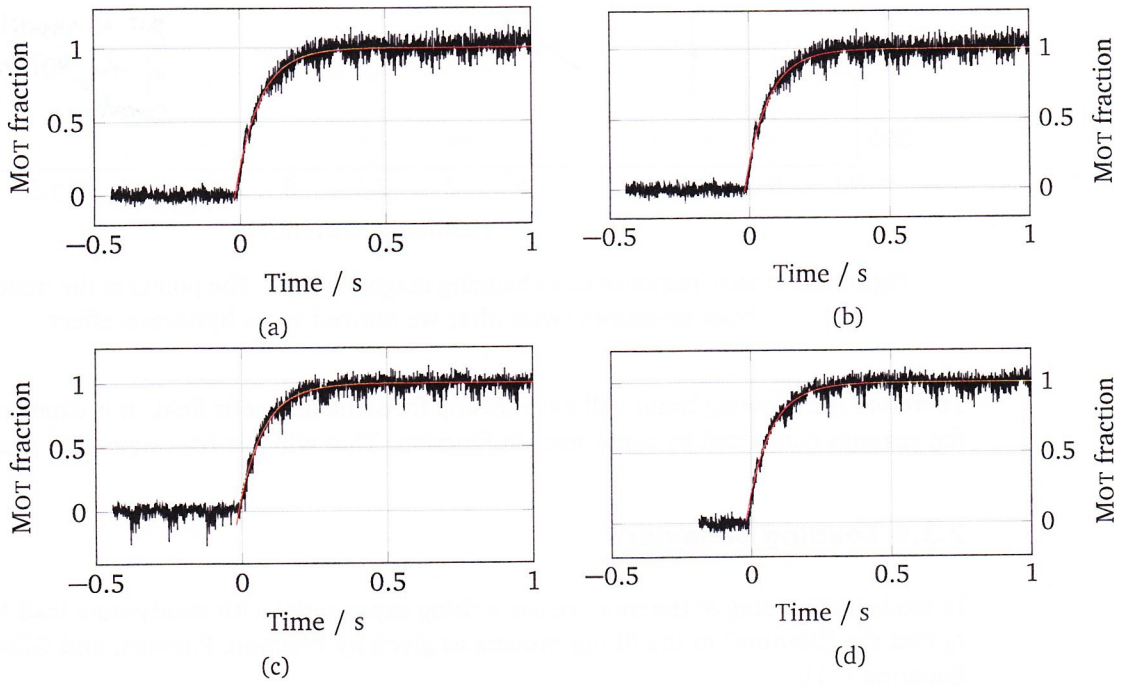

Figure 2.15: Repeated measurement of the MOT loading time. The signal of the photodiode is voltage measured at the oscilloscope. We have rescaled the signal such that no MOT is around zero and with MOTit is around unity. We have also shifted it such that $t_0 = 0$ for better comparison. In red the rising exponential fit is shown.

The time constant τ is the inverse of the scattering rate. In our case we can ignore the background atoms and assume that the scattering only happens with the rubidium atoms. Therefore Equation (2) in the paper of Wieman, Flowers, and Gilbert [WFG95] reduces to

$$\tau^{-1} = n\sigma v\,.$$

We want to compute the cross section. Therefore we need the number density n and the velocity v. The average velocity of the thermal distribution will suit our needs here. It is given by

$$v = \sqrt{\frac{2k_\mathrm{B}T}{m}} = 170\,\mathrm{m\,s^{-1}}\,,$$

where $m = 1.41 \times 10^{-25}\,\mathrm{kg}$ is the mass of rubidium atoms [WFG95, p. 320]. The density n can be computed using

$$n = \frac{P}{k_\mathrm{B}T} = 3.2(5) \times 10^{15}\,\mathrm{m^{-3}}\,.$$

Solving the above equation for the cross section σ, we obtain

$$\sigma = \frac{1}{\tau n v} = 2.1(3) \times 10^{-17}\,\mathrm{m^2}\,.$$

3 Conclusion

In this experiment we built up a MOT by adjusting the mirrors and $\lambda/2$ plates on the given setup. We were able to achieve a MOT power of around 192(19) nW with our configuration. This is much higher than needed, which is good.

Then by measuring the cooling laser beam intensity and diameter we were able to compute the beam intensity and the cooling scattering rate. By measuring the detuning of the cooling laser we were able to estimate the number of atoms in our MOT to be $2.0(5) \times 10^7$.

The volume of our MOT is $26.3\,\mathrm{mm}^3$, determined from a photo taken with a camera.

The loading behavior has a time constant of $\tau = 0.087(4)\,\mathrm{s}$. From that we were able to compute the cross section of scattering with background rubidium gas go be $2.1(3) \times 10^{-17}\,\mathrm{m}^2$. This is a sensible result as the diameter of the hydrogen atom is around $10^{-10}\,\mathrm{m}$. Rubidium will be somewhat larger. Taking the square of this diameter will give a ballpark estimation of the cross section as we assume short-range scattering.

The large errors on our measurements mostly stem on from the uncertainty of the distance between the MOT and the lens which projects the MOT onto the power meter. Also the pressure was not known precisely. All in all we only get one significant digit for most derived quantities. If there would be a way to get a better position measurement of the lens, all errors could be reduced significantly.

It was nice to have an oscilloscope which would write the raw data to the USB thumbdrive. That way we could extract the loading time from the raw measurements and did not have to twiddle with an exported image of the oscillogram.

Note: 1,0

Bibliography

[WFG95] Carl Wieman, Gwenn Flowers, and Sarah Gilbert. "Inexpensive laser cooling and trapping experiment for undergraduate laboratories". In: *American Journal of Physics* 63.4 (Apr. 1995), pp. 317–329. URL: http://web.pdx.edu/~larosaa/Applied_Optics_464-564/Projects_Presented/Projects-2006/Laser%20Cooling/Am%20J%20Phys%2063,%20317.pdf.